ACIS Spatial Contamination Effects

There is a layer of X-ray absorbing contaminant deposited on the ACIS filters. It has transmission strongly dependent on wavelength, is changing with time, and is non-uniformly distributed. Details regarding characterization and calibration of the effect can be found on the CXC Calibration Group web pages.[1]

In CIAO 3.2 and Calibration Database version 3.0, we have implemented a spatial contamination model which supersedes the uniform contaminant model. The CALDB file structure and functional form are defined in the "Analysis Reference Data Interface Control Document."[2]

No explicit changes to response generation are needed to apply the spatial contaminant response. The interface, via "`ardlib`" is implicit in the CIAO response programs, `mkarf`, `mkgarf`, and `mkinstmap`. There are new `ardlib` parameters and qualifiers for explicit control. See the appropriate CIAO help pages for details. Further information can be found on the CXC CALDB web pages.[3]

Here we reiterate the contamination function, and then show the effects on responses for nominal instrumental configurations relative to the uniform contaminant model. The new calibration file is `acisD1999-08-13contamN0004.fits`, which we compare to the uniform contaminant model of `acisD1999-08-13contamN0003.fits`. Both files can be found in the CALDB subdirectory, `$CALDB/data/chandra/acis/bcf/contam/`.

The Contamination Function

The transmission efficiency of N contaminants, i, in M partial covering regions, j, can be expressed as

$$\epsilon(E,t,x,y) = \sum_{j=1}^{M} F_j e^{-\kappa_j \sum_{i=1}^{N} \mu_{ij}(E)\,\tau_{ij}(t,x,y)} \tag{1}$$

in which the relative thickness as a function of position and time is

$$\tau_{ij}(t,x,y) = \tau_{0ij}(t-t_0) + \tau_{1ij}(t-t_0) f_{ij}(x,y). \tag{2}$$

Here E is photon energy in keV, t is time in seconds since the reference time, t_0, $\mu(E)$ is the relative absorption coefficient per unit thickness, τ are the relative thicknesses of the contaminants, and $f(x,y)$ defines the spatial distribution. The reference time, t_0, is the *Chandra* `MJDREF`, 50814.0 (1998.0). The absorption coefficient and thicknesses are in relative units since their absolute values are not known. Their product yields an observable optical depth.

[1] "Spatial structure in the ACIS OBF contamination" (A. Vikhlinin, 5/09/04; `http://cxc.harvard.edu/contrib/alexey/cont_spat.pdf`)

[2] `http://space.mit.edu/ASC/docs/ARD_ICD/ARD_ICD-v1.7_contamxy.ps.gz`

[3] `http://cxc.harvard.edu/ciao/why/acisqedeg.html`

The total absorption optical depth for N contaminants is given by the sum of individual optical depths over index i. The sum over j allows an option for partial filling factors by different contaminants, with weights F_j and κ_j.

There is a dependence upon the ACIS CCD, primarily upon the read-out array, ACIS-I or ACIS-S (since they have different thermal loading). For generality in chip-to-chip differences, there is one FITS binary table extension per CCD.

The calibration file tabulates F, κ, $\mu(E)$, $\tau(t)$, $f(x, y)$, t, and E.

Grating Response/ACIS-S

A recent calibration observation used to characterize the contaminant was of Markarian 421 made with LETG/ACIS-S on July 12, 2004 (ObsID 5331). In Figure 1, the top panel shows the effective areas for no contamination (grey; highest curve), the uniform spatial model (red; middle curve), and the new spatially dependent model (blue; lowest curve).

The lower panel shows the ratios of each of the old and the new models to the uncontaminated response (red and blue, respectively). The x coordinate is $m\lambda$, and only ± 1 orders are shown. This test was used for verification by the Calibration Group. It include bad pixels and dither.

Figures 2–4 show the ratios of the new model to the uniform model at different times for LETG/ACIS-S, MEG/ACIS-S, and HEG/ACIS-S. Curves from top to bottom are at different epochs (though the latest three largely overlap). The approximate zero order `CHIPY` is given in the plot title, and is the nominal offset for the each configuration (-3mm for HETG, and -9mm for LETG). No dither was included in these responses so the chip gaps show as sharp discontinuities. Since the HETG spectra traverse a large range in `CHIPY`, the HETG (HEG and MEG) responses are asymmetric in positive and negative orders. There is little overall effect at the HEG energies, but much for LEG.

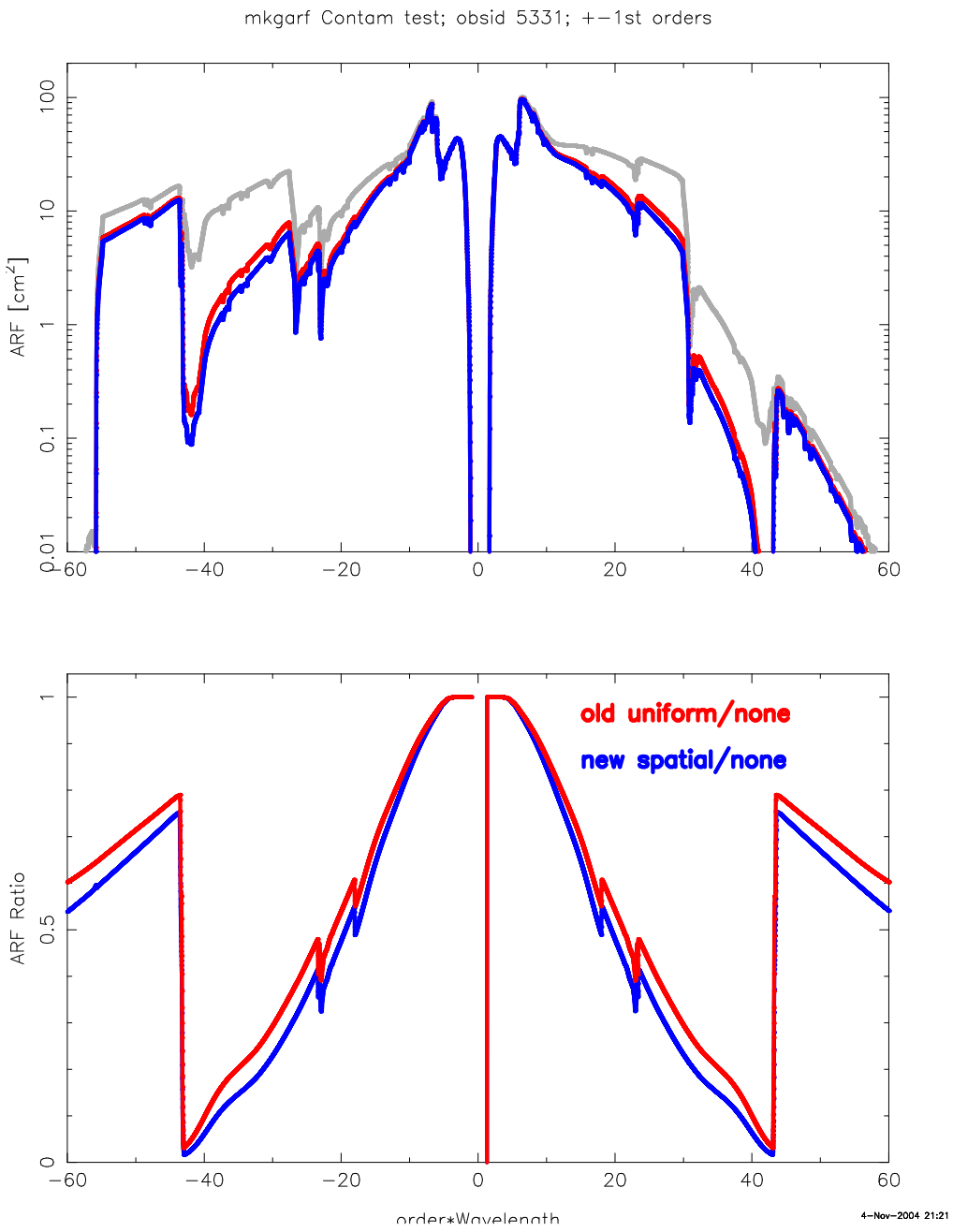

Figure 1: The effective area function (top) and ratios (bottom) for the observation of Markarian 421 made with LETG/ACIS-S on July 12, 2004 (ObsID 5331).

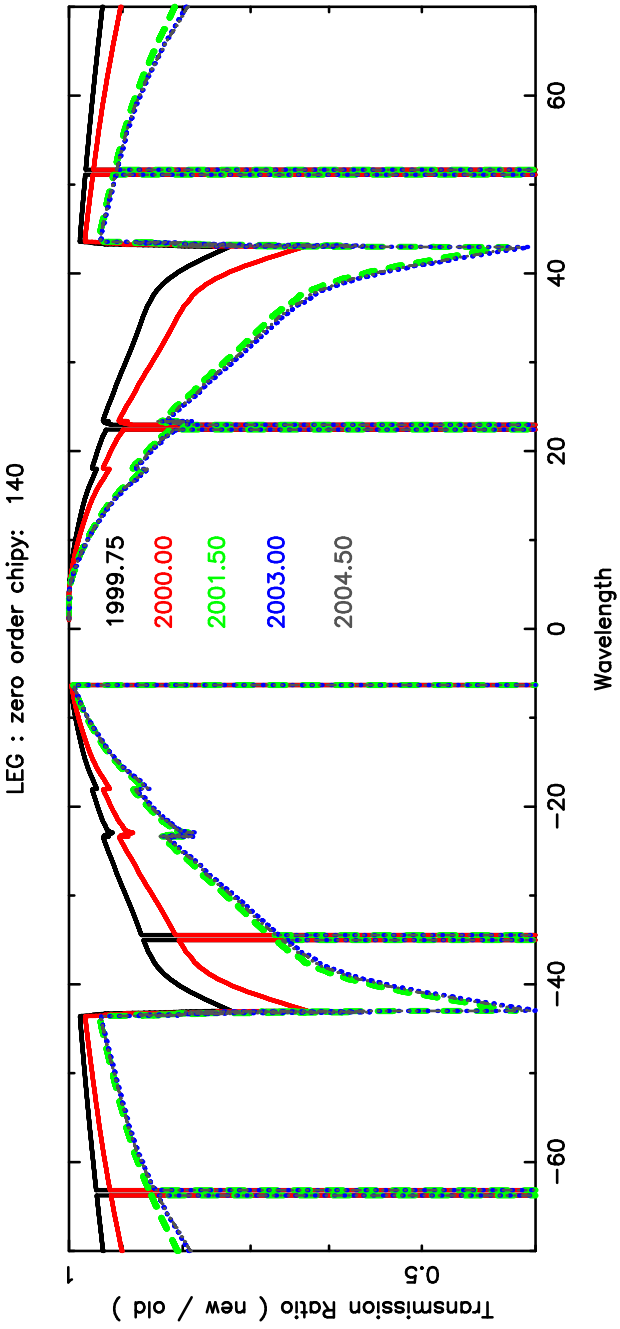

Figure 2: The ratio of the new model to the uniform model at different times for LEG/ACIS-S.

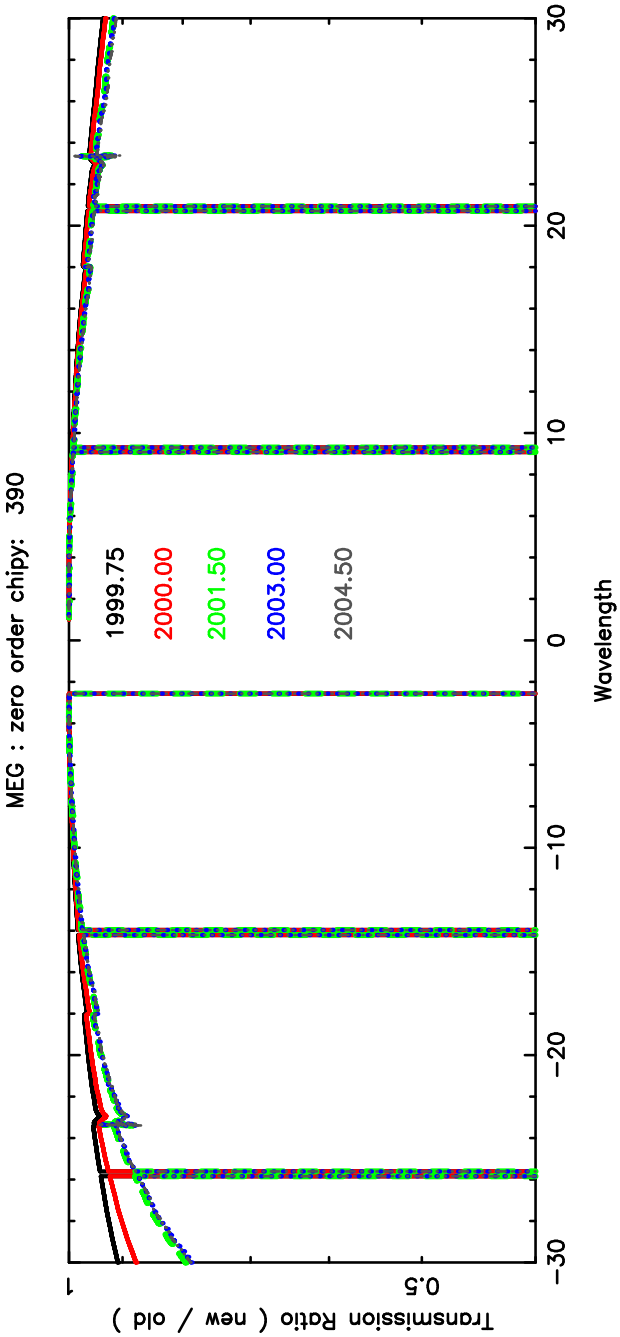

Figure 3: The ratio of the new model to the uniform model at different times for MEG/ACIS-S).

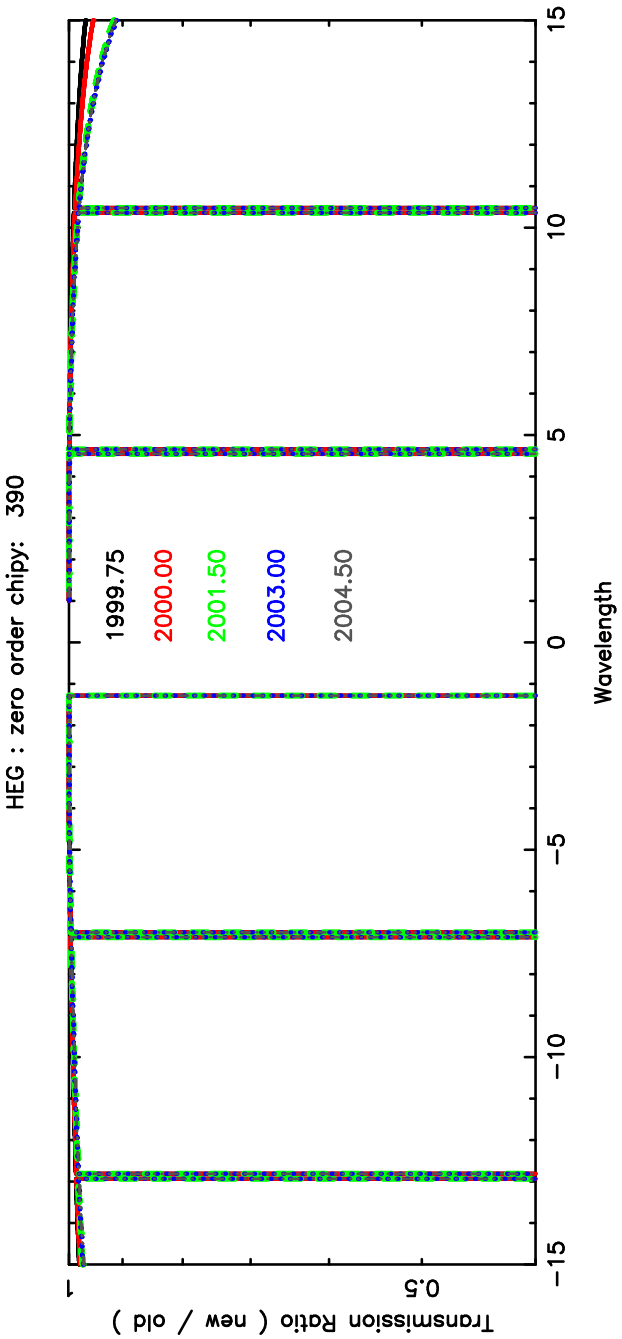

Figure 4: The ratio of the new model to the uniform model at different times for HEG/ACIS-S.

Imaging Response/ACIS-I/ACIS-S3

The non-uniform spatial distribution of the contaminant is determined by the temperature of the ACIS filter. The detectors and filters are cooled by thermoelectric devices around their perimeter. For ACIS-I, this leads to a radial pattern in contaminant thickness. For ACIS-S, it depends only on `CHIPY`.

Figure 5 shows one chip from ACIS-I, I-2 (`CCD_ID` = 2). There is about a 20% gradient in response from center to edge. Figure 6 shows the ACIS-S3 (`CCD_ID` = 7) contamination map; the value near the center is about 0.8, and is about 0.6 near the edge.

Figures 7–8 show the effective areas and for new and old contamination models, and their ratios.

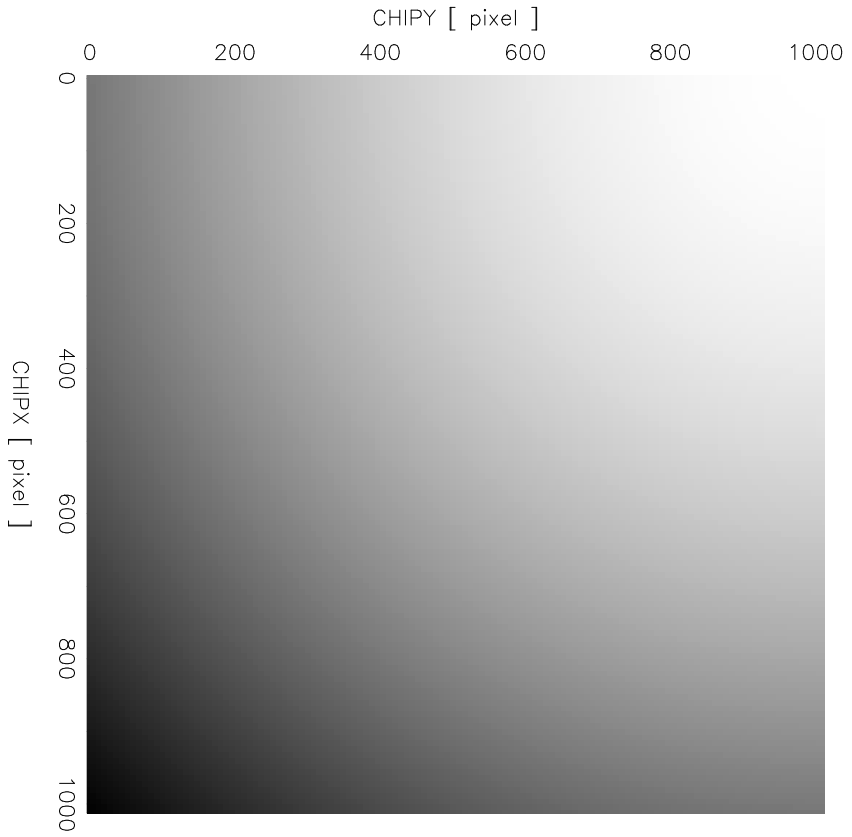

Figure 5: The ACIS-2 (I2) instrument map at 1 keV for contamination only (mirror area= 1, $QE = 1$) in mid-2004. The transmission in the upper right is 0.8, and at the lower left is 0.6.

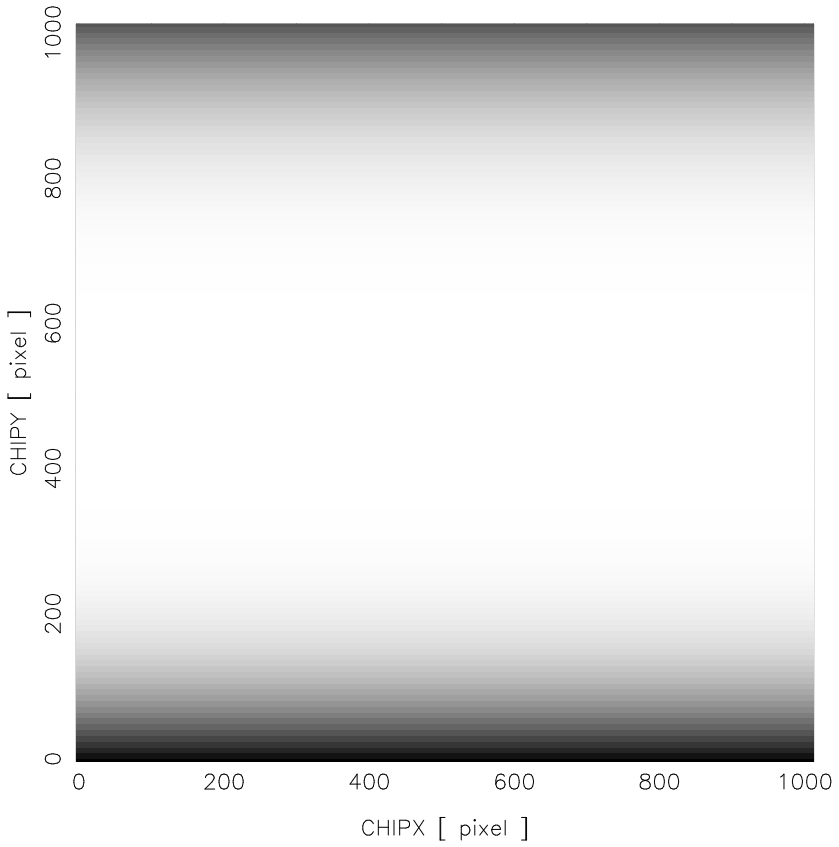

Figure 6: The ACIS-7 (S3) instrument map at 1 keV for contamination only (mirror area= 1, $QE = 1$) in mid-2004. The transmission in the center is 0.8, and at the lower edge is 0.6.

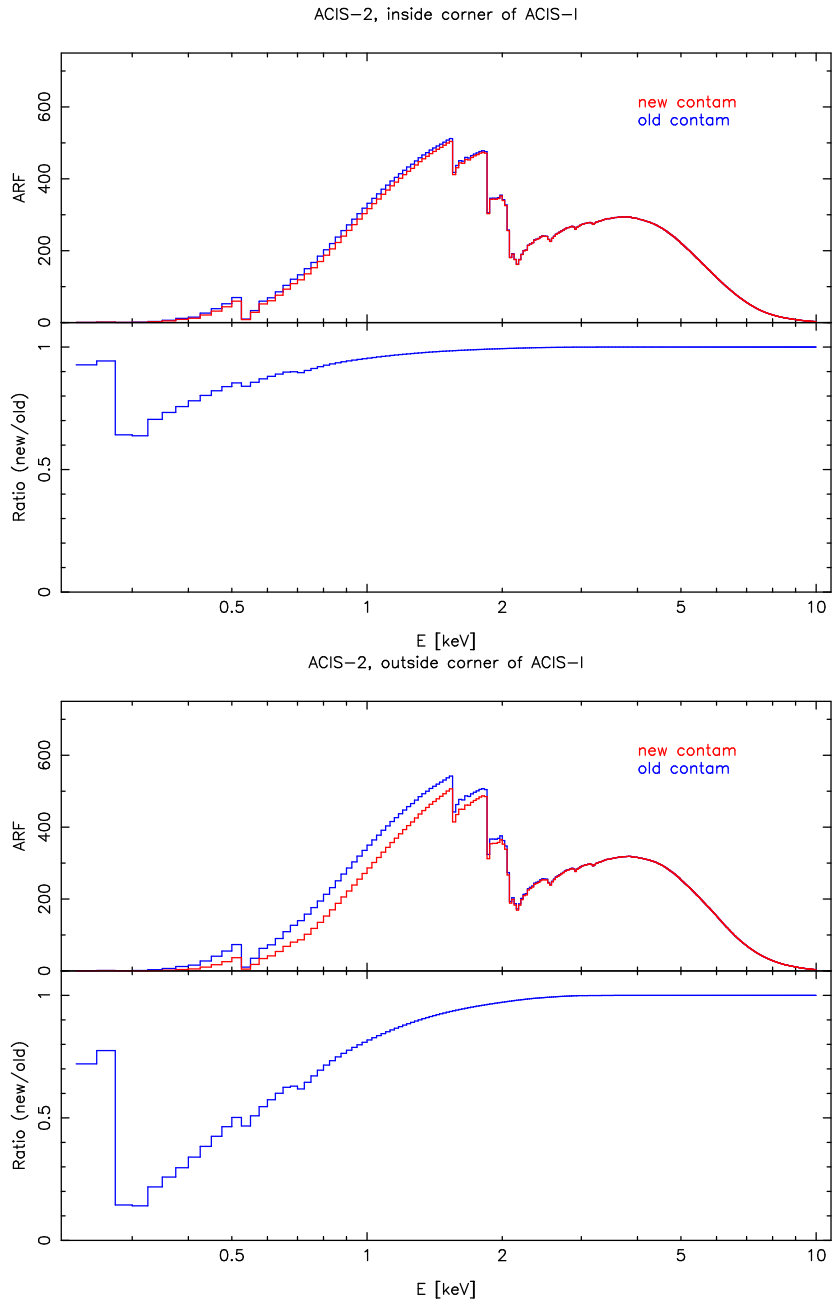

Figure 7: The ACIS-2 (I2) effective area in mid-2004 for the spatial and uniform contamination models near the ACIS-I center (top), and near the edge (bottom). In each plot, the top panel is the effective area, and the bottom the ratio of the new (spatially dependent) to old (uniform) contamination models.

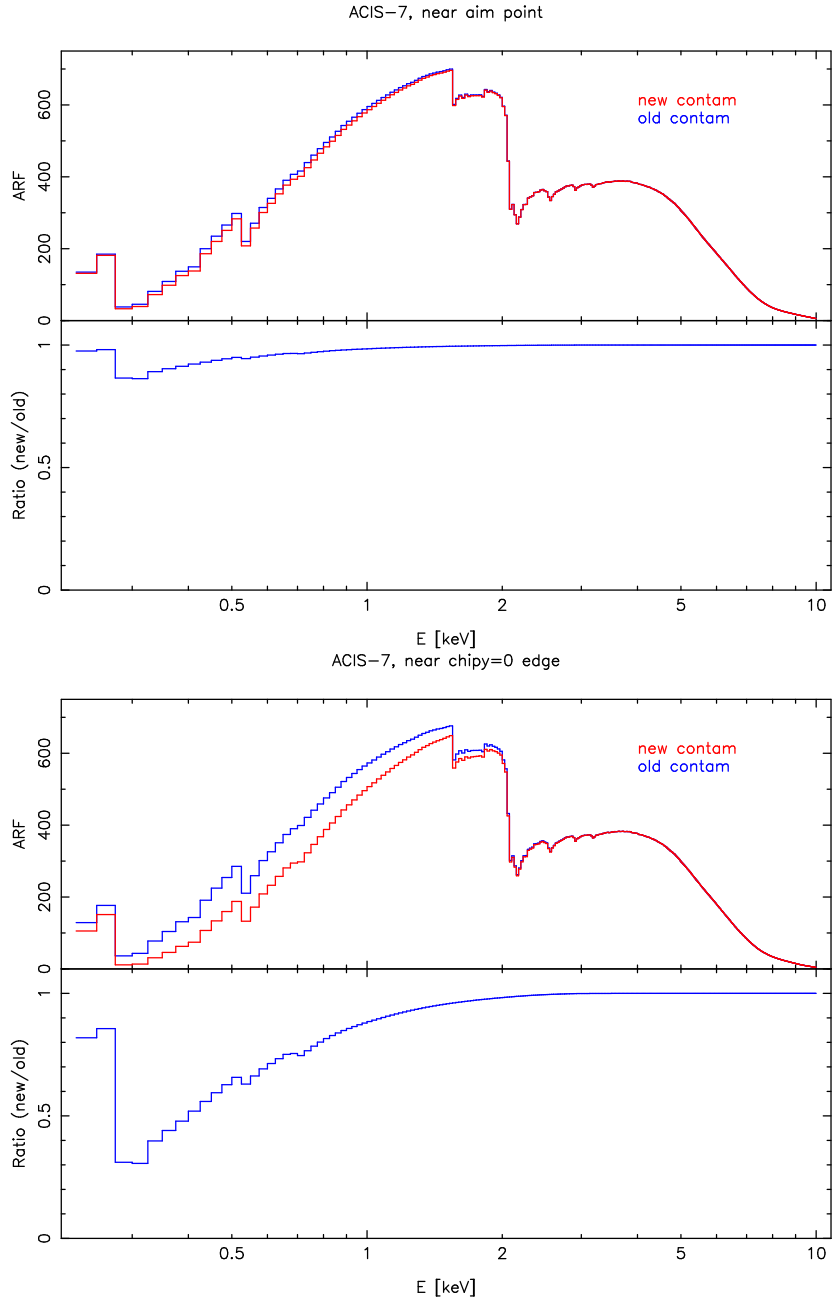

Figure 8: The ACIS-7 (S3) effective area in mid-2004 for the spatial and uniform contamination models. Top plot is the response evaluated near the aim point of S3 on the ACIS-S array, and the lower plot is near the edge. In each plot, the upper panel is the effective area, and the lower is the ratio of new spatially dependent model to the old uniform model.